Iran J Sci Technol Trans Sci
https://doi.org/10.1007/s40995-021-01235-9

RESEARCH PAPER

A Reliable Explicit Method to Approximate the General Type of the KdV–Burgers' Equation

Sıla Övgü Korkut[1] · Neslişah İmamoğlu Karabaş[2]

Received: 7 June 2021 / Accepted: 10 October 2021

Abstract
This study aims to propose a reliable, accurate, and efficient numerical approximation for a general compelling partial differential equation including nonlinearity $\left(u^{\delta}\frac{\partial u}{\partial x}\right)$, dissipation $\left(\frac{\partial^2 u}{\partial x^2}\right)$, and dispersion $\left(\frac{\partial^3 u}{\partial x^3}\right)$ which arises in many fields of engineering as well as applied sciences. The novel proposed method has been developed combining a kind of mesh-free method called the Taylor wavelet method with the Euler method. The convergence result of the method has been presented theoretically. Moreover, the validation and applicability of the method have been also confirmed computationally on benchmark problems such as KdV–Burgers' equation and modified-KdV equation. The numerical results have been compared both to the exact solution and to those in the existing literature. All presented figures and tables guarantee that the proposed method is highly accurate, efficient, and compatible with the nature of the specified equation physically. Furthermore, the recorded errors are evidence that the proposed method is the best approximation compared to those in the existing methods.

Keywords KdV–Burgers' equation · Modified-KdV equation · Taylor wavelet · Nonlinearity

1 Introduction

Due to the nonlinearity of nature, many natural processes arising in several fields of sciences, such as wave propagation phenomena, fluid mechanics, plasma physics, quantum mechanics, nonlinear optics, chemical kinematics, possessing a complex phenomenon are modeled by nonlinear partial differential equations. To understand the existing truth behind these processes and to make inferences for future estimation, the model is required to solve numerically or analytically. However, these models can contain combinations of dissipation and dispersion as well as nonlinearity. This makes a numerical scheme more challenging to catch the physical behavior and, therefore, developing a numerical method more attractive.

In this study, we mainly focus on the following partial differential equation which contains dissipation $\left(\frac{\partial^2 u}{\partial x^2}\right)$, dispersion $\left(\frac{\partial^3 u}{\partial x^3}\right)$ and nonlinearity $\left(u^{\delta}\frac{\partial u}{\partial x}\right)$ such that

$$\frac{\partial u}{\partial t}+\alpha u^{\delta}\frac{\partial u}{\partial x}-\beta\frac{\partial^2 u}{\partial x^2}+\gamma\frac{\partial^3 u}{\partial x^3}=0,\quad x\in\Omega=(a,b),\ t>0$$

subject to the following boundary conditions for $\alpha,\ \beta,$ and $\gamma\in\mathbb{R}$

$$\begin{aligned} &u(x=a,t)=g_0(t),\\ &u(x=b,t)=g_1(t),\\ &\frac{\partial u}{\partial x}(x=a,t)=f(t), \end{aligned} \tag{1}$$

where the initial condition is

$$u(x,0)=u_0(x),\ x\in\Omega. \tag{2}$$

The specified equation is called Kortweg-de Vries–Burger type for $\delta=1$. It reduces to the Burgers' equation for the case of $\delta=1$ and $\gamma=0$. Moreover, for the choice of $\delta=1$, and $\beta=0$ the equation returns to Kortweg-de Vries (KdV) equation. One can, further, obtain the modified Kortweg-de

✉ Sıla Övgü Korkut
silaovgu@gmail.com

[1] Department of Engineering Sciences, Izmir Katip Celebi University, Izmir, Turkey

[2] Department of Mathematics, Izmir Institute of Technology, Izmir, Turkey

Published online: 15 November 2021

Vries (mKdV) when the parameters are taken as $\delta = 2$, and $\beta = 0$.

A lot of effort has been invested into construct to approximate the solution of such equations in the literature. Some of these valuable studies can be summarized as follows: in Shi et al. (2015) a hybrid scheme based on higher compact order compact scheme and classical constraint interpolation profile has been proposed. Aydın has applied an unconventional splitting method for solving the Korteweg de Vries–Burgers equation in Aydin (2015). The Crank–Nicolson method combined with a mesh-free method based on radial basis functions has been suggested in Haq et al. (2009) and with the Galerkin finite element method by using quintic B-splines has been given in Irk (2017). For the KdV–Burgers equation, Darvishi et al. have proposed an approximate solution based on spectral collocation points and the 4th-order Runge–Kutta method (RK4) in Darvishi et al. (2007). Motsa et al. have suggested a new method which combines quasilinearization, the Chebyshev spectral collocation method, and bivariate Lagrange interpolation to solve nonlinear partial differential equation including both modified KdV–Burgers equation and modified KdV equation in Motsa et al. (2014). Moreover, semi-analytical methods including homotopy analysis method, homotopy perturbation method, Adomian decomposition method, and variational iteration method have been discussed for both KdV and modified KdV equation in Kaya (2009). A Haar wavelet approach has been studied for the numerical solution of modified KdV and modified Burgers' equation in Ray and Gupta (2015). An approach based on a lumped Galerkin method via cubic B-spline interpolation has been proposed for the modified KdV equation in Ak et al. (2017). Furthermore, more recently, a mesh-free method combined with the exponential Rosenbrock method has been suggested in Koçak (2021) for solving the KdV–Burgers equation. The specified equation is also solved numerically by an extended B-spline collocation method combined with the RK4 in Hepson et al. (2019). A higher-order Haar wavelet method via ODE45 solver in MATLAB has been applied to both Burgers' equation and KdV equation in Ratas and Salupere (2020). The Haar wavelet method has been used to solve KdV-type partial differential equations of order seven in Saleem et al. (2021).

As presented above, various valuable studies have already been worked for the specified equations. However, it, of course, continues to be an area of interest of the researchers for whom to enrich a deep understanding of such attractive equations. The focus point of this study is to develop a numerical scheme based on the Taylor wavelet collocation method presented in Keshavarz et al. (2018) for solving both the KdV–Burgers' and modified KdV equations. The wavelet methods which have become more popular in recent years have been used for solving various kinds of differential equations, (Dehestani et al. 2019, 2021a, b, c; Kumar and Priyadarshi 2018; Priyadarshi and Kumar 2020). However, to the authors' best knowledge, the current study is the first time that the Taylor wavelet collocation method has been proposed to solve both modified KdV and KdV–Burgers' equations. Moreover, the other originality of the current study is that unlike the aforementioned studies based on the wavelet approximation considering for the general domain instead of (0, 1). Furthermore, the current work has also aimed to be the first study to present the CPU time for the considered KdV–Burgers' type equation.

Motivated by these aims, the rest of the paper has the following structure. Section 2 aims to describe the numerical scheme as well as the Taylor wavelet method. This section is followed by a more theoretical section, Sect. 3, which analyzes the convergence of the proposed scheme. The validity, efficiency, and applicability of the proposed method are discussed in Sect. 4 by presenting evidence with tables and figures. The study is concluded by emphasizing some important comments and discussions in Sect. 5.

2 Numerical Method

The main objective of this section is to share the method in a brief and understandable way with the readers. That's why the section is divided into two subsections. The upcoming section presents an introduction to the Taylor wavelet method and its integral forms. It is followed by the construction of the proposed numerical scheme.

2.1 Taylor Wavelet Method

One of the important classes of wavelet methods is the Taylor wavelet which is defined by Keshavarz et al. Keshavarz et al. (2018). Let $n = 1, 2, \ldots, 2^{k-1}$ for $k \in \mathbb{Z}^+$ and m be a non-negative integer, then the Taylor wavelets on the interval [0, 1) are defined as follows:

$$\psi_{nm}(x) = \begin{cases} 2^{\frac{k-1}{2}} \hat{T}_m\left(2^{k-1}x - n + 1\right), & \text{if } \dfrac{n-1}{2^{k-1}} \leq x < \dfrac{n}{2^{k-1}}, \\ 0, & \text{otherwise}, \end{cases} \tag{3}$$

where $\hat{T}_m$ for $m = 0, 1, 2, \ldots, M-1$ denotes the normalized Taylor polynomial of degree m such that $\hat{T}_m(x) = \sqrt{2m+1}x^m$. Thus, any function $f(x) \in L^2[0, 1]$ can be expanded in terms of the Taylor wavelets as follows:

$$f(x) = \sum_{n=1}^{\infty} \sum_{m=0}^{\infty} c_{nm} \psi_{nm}(x). \tag{4}$$

Here c_{nm} stands for the Taylor wavelet coefficients and are determined by

$$c_{nm} = \langle f(x), \psi_{nm}(x) \rangle,$$

where $\langle \cdot, \cdot \rangle$ the inner product. It is crucial to remind that by the orthonormality property $\langle \psi_{nm}(x), \psi_{nm}(x) \rangle = 1$. By utilizing the truncated form of the infinite series in Eq. (4), the approximation of $f(x)$ can be expressed by

$$f(x) \simeq \sum_{n=1}^{2^{k-1}} \sum_{m=0}^{M-1} c_{nm} \psi_{nm}(x) = \mathbf{C}\mathbf{\Psi}(x), \tag{5}$$

where

$$\begin{aligned} \mathbf{C} = \big[& c_{10}, c_{11}, \ldots, c_{1(M-1)}, c_{20}, c_{21} \ldots, c_{2(M-1)}, \\ & \ldots c_{2^{k-1}0}, c_{2^{k-1}1}, \ldots, c_{2^{k-1}(M-1)} \big], \end{aligned} \tag{6}$$

and

$$\mathbf{\Psi}(x) = \begin{bmatrix} \psi_{10}(x_0) & \psi_{10}(x_1) & \cdots & \psi_{10}\left(x_{2^{k-1}(M-1)}\right) & \psi_{10}\left(x_{2^{k-1}(M)}\right) \\ \psi_{11}(x_0) & \psi_{11}(x_1) & \cdots & \psi_{11}\left(x_{2^{k-1}(M-1)}\right) & \psi_{11}\left(x_{2^{k-1}(M)}\right) \\ \vdots & & \cdots & & \vdots \\ \psi_{2^{k-1}(M-1)}(x_0) & \psi_{2^{k-1}(M-1)}(x_1) & \cdots & \psi_{2^{k-1}(M-1)}\left(x_{2^{k-1}(M-1)}\right) & \psi_{2^{k-1}(M-1)}\left(x_{2^{k-1}(M)}\right) \end{bmatrix} \tag{7}$$

where $M-1$ is the highest degree of the polynomial. On the other hand, the general integral form of the Taylor wavelets can be defined as follows:

$$I^p \psi_{nm}(x) = \begin{cases} 0, & \text{if} 0 \le x < \dfrac{n-1}{2^{k-1}}, \\ \dfrac{2^{\left(m+\frac{1}{2}\right)(k-1)} m! \sqrt{2m+1}}{(m+p)!} \left(x - \dfrac{n-1}{2^{k-1}} \right)^{m+p}, & \text{if} \dfrac{n-1}{2^{k-1}} \le x < \dfrac{n}{2^{k-1}}, \\ \dfrac{2^{\left(m+\frac{1}{2}\right)(k-1)} m! \sqrt{2m+1}}{(m+p)!} \left(x - \dfrac{n-1}{2^{k-1}} \right)^{m+p} - A(x), & \text{if} \dfrac{n}{2^{k-1}} \le x \le 1, \end{cases} \tag{8}$$

where p represents the positive integer and it is taken specifically as $p = 1, 2, 3$ in the current study. Moreover,

$$A(x) = \sum_{j=0}^{m} \binom{m}{j} \frac{2^{\left(j+\frac{1}{2}\right)(k-1)} j! \sqrt{2m+1}}{(j+p)!} \left(x - \frac{n}{2^{k-1}} \right)^{j+p}. \tag{9}$$

Our general references on Taylor wavelets and their integral forms are (Vichitkunakorn et al. 2020; Keshavarz et al. 2018; Keshavarz and Ordokhani 2019).

2.2 Method of Solution

The current section aims to present the proposed method in an understandable language. To adapt the Taylor wavelet method for solving the equation given in Eqs. (1), (2), the physical domain is required to transform from $[a, b]$ into $[0, 1]$. To do this, define $X = \frac{x-a}{\hbar}$ where $\hbar = b - a$, then Eq. (1) returns to

$$\begin{aligned}
&\frac{\partial w}{\partial t}+\frac{\alpha}{\hbar}w^{\delta}\frac{\partial w}{\partial X}-\frac{\beta}{\hbar^2}\frac{\partial^2 w}{\partial X^2}+\frac{\gamma}{\hbar^3}\frac{\partial^3 w}{\partial X^3}=0, \quad X\in(0,1),\ t>0,\\
&w(0,t)=g_0(t),\\
&w(1,t)=g_1(t),\\
&\frac{\partial w}{\partial X}(0,t)=f_{\hbar}(t),\\
&w(X,0)=w_0(X),\ X\in(0,1).
\end{aligned} \tag{10}$$

where $w(X,t)=u(x,t)$. Notice that $f_{\hbar}(t)=\hbar f(t)$.

Consider Eq. (10), the numerical solution can be obtained with the help of the Taylor wavelet method as follows:

$$\frac{\partial^4 w}{\partial t\partial X^3}(X,t)\simeq\sum_{n=1}^{2^{k-1}}\sum_{m=0}^{M-1}c_{nm}(t)\psi_{n,m}(X)=\mathbf{C}(t)\Psi(X). \tag{11}$$

Define $t_r=r\Delta t$ such that $\Delta t=\frac{t_{\text{final}}}{N}$ where N is the number of divisions of the time interval. To describe the numerical solution, we first, integrate Eq. (11) over the interval $[t_r,t]$ with respect to t. Then, we have

$$\int_{t_r}^{t}\frac{\partial^4 w}{\partial s\partial X^3}(x,s)\,\mathrm{d}s\simeq\int_{t_r}^{t}\mathbf{C}(s)\Psi(x)\mathrm{d}s, \quad t\in[t_r,t_{r+1}]. \tag{12}$$

Let $W(x,t)$ denote the approximate solution. Due to the non-availability of $\mathbf{C}(s)$ we write the integral given in Eq. (12) using the left-hand point approximately. Therefore,

$$\frac{\partial^3 W}{\partial X^3}(x,t)=(t-t_r)\boldsymbol{C}_r\Psi(X)+\frac{\partial^3 W}{\partial X^3}(X,t_r), \quad t\in[t_r,t_{r+1}], \tag{13}$$

where $\boldsymbol{C}_r$ and $\Psi(X)$ are defined in Eqs. (6) and (8), respectively. Notice that, for the sake of simplicity of notations $\boldsymbol{C}_r$ stands for $\mathbf{C}(t_r)$ throughout the section. Notice that Eq. (13) is independent of the time variable. To describe the numerical solution, we integrate Eq. (13) with respect to X over the interval $[0,X]$,

$$\begin{aligned}
\frac{\partial^2 W}{\partial X^2}(X,t)&=(t-t_r)\boldsymbol{C}_r\boldsymbol{I^1}\boldsymbol{\Psi}(X)+\frac{\partial^2 W}{\partial X^2}(X,t_r)\\
&+\underbrace{(W_{XX}(0,t)-W_{XX}(0,t_r))}_{①},
\end{aligned} \tag{14}$$

$$\begin{aligned}
\frac{\partial W}{\partial X}(X,t)&=\frac{\partial W}{\partial X}(X,t_r)+(t-t_r)\boldsymbol{C}_r\boldsymbol{I^2}\boldsymbol{\Psi}(X)\\
&+\left(\frac{\partial W}{\partial X}(0,t)-\frac{\partial W}{\partial X}(0,t_r)\right)\\
&+X\underbrace{\left(\frac{\partial^2 W}{\partial X^2}(0,t)-\frac{\partial^2 W}{\partial X^2}(0,t_r)\right)}_{①},
\end{aligned} \tag{15}$$

$$\begin{aligned}
W(X,t)&=W(X,t_r)+W(0,t)-W(0,t_r)\\
&+(t-t_r)\boldsymbol{C}_r\boldsymbol{I^3}\boldsymbol{\Psi}(X)\\
&+X\left(\frac{\partial W}{\partial X}(0,t)-\frac{\partial W}{\partial X}(0,t_r)\right)\\
&+\frac{X^2}{2}\underbrace{\left(\frac{\partial^2 W}{\partial X^2}(0,t)-\frac{\partial^2 W}{\partial X^2}(0,t_r)\right)}_{①},
\end{aligned} \tag{16}$$

where $\boldsymbol{I^p}\boldsymbol{\Psi}(X)$ for $p=1,2,3$ stands for the integral form of the Taylor method given in Eq. (8). Before proceeding to detailed calculations, it is worth noting that

$$\begin{aligned}
&W(X,0)=w_0(X),\\
&\frac{\partial^2 W}{\partial X^2}(X,0)=\hbar^2 w_0''(X),
\end{aligned} \tag{17}$$

Moreover, for the sake of simplicity of the exposition, we use $(f_{\hbar})_r^t$, $(g_1)_r^t$, and $(g_0)_r^t$ to abbreviate $f_{\hbar}(t)-f_{\hbar}(t_r)$, $g_1(t)-g_1(t_r)$, and $g_0(t)-g_0(t_r)$, respectively. Notice that all terms in Eqs. (13)–(16) can be expressed in terms of initial and boundary conditions except ①. By substituting $x=1$ one can be obtained from Eq. (15) that

$$\text{◯I}=\underbrace{\frac{\partial W}{\partial X}(1,t)-\frac{\partial W}{\partial X}(1,t_r)}_{①\!\!①}-f_{\hbar_r}^t-(t-t_r)\boldsymbol{C}_r\boldsymbol{I^2}\boldsymbol{\Psi}(1). \tag{18}$$

By putting Eq. (18) into Eq. (16), one can express

$$\begin{aligned}
W(X,t)&=W(X,t_r)+(g_0)_r^t+(t-t_r)\boldsymbol{C}_r\boldsymbol{I^3}\boldsymbol{\Psi}(X)+X\left((f_{\hbar})_r^t\right)\\
&+\frac{X^2}{2}\left(\underbrace{\frac{\partial W}{\partial X}(1,t)-\frac{\partial W}{\partial X}(1,t_r)}_{①\!\!①}-f_{\hbar_r}^t-(t-t_r)\boldsymbol{C}_r\boldsymbol{I^2}\boldsymbol{\Psi}(1)\right).
\end{aligned} \tag{19}$$

After substituting $x=1$ in the above-mentioned equation, and doing the required calculations, we have

$$\begin{aligned}
①\!\!①&=2\left[(g_1)_r^t-(g_0)_r^t-(f_{\hbar})_r^t-(t-t_r)\boldsymbol{C}_r\boldsymbol{I^3}\boldsymbol{\Psi}(1)\right]\\
&+(f_{\hbar})_r^t+\boldsymbol{C}_r\boldsymbol{I^2}\boldsymbol{\Psi}(1).
\end{aligned} \tag{20}$$

Furthermore, to construct the final form of the numerical scheme one more expression, $\frac{\partial W}{\partial t}$, is required to define. For

this purpose, Eq. (16) is derived with respect to t as follows:

$$\frac{\partial W}{\partial t}(X,t) = \boldsymbol{C}_r \boldsymbol{I}^3 \boldsymbol{\Psi}(X) + X\left(\frac{\partial}{\partial t}\left(\frac{\partial W}{\partial X}\right)_{(0,t)}\right) + \frac{X^2}{2}\left(\frac{\partial}{\partial t}\left(\frac{\partial^2 W}{\partial X^2}\right)_{(0,t)}\right) + \frac{\partial W}{\partial t}(0,t). \tag{21}$$

To avoid derivatives on the boundary conditions, we utilize the definition of the derivative. That is, $\frac{\partial}{\partial t}\left(\frac{\partial^2 W}{\partial X^2}\right)(0,t) \approx \frac{\frac{\partial^2 W}{\partial X^2}(0,t) - \frac{\partial^2 W}{\partial X^2}(0,t_r)}{t - t_r}$. Likewise, $\frac{\partial W}{\partial t}(0,t)$ and $\frac{\partial}{\partial t}\left(\frac{\partial W}{\partial X}\right)(0,t)$ can be also obtained. Then, Eq. (21) can be expressed by assuming $t \to t_{r+1}$ as follows:

$$\frac{\partial W}{\partial t}(X,t_{r+1}) = \boldsymbol{C}_r \boldsymbol{I}^3 \boldsymbol{\Psi}(X) + X\left(\frac{(f_\hbar)_r^{r+1}}{\Delta t}\right) + \frac{X^2}{2}\left(2\frac{(g_1)_r^{r+1} - (g_0)_r^{r+1} - (f_\hbar)_r^{r+1} - \Delta t \boldsymbol{C}_r \boldsymbol{I}^3 \boldsymbol{\Psi}(1)}{\Delta t}\right). \tag{22}$$

Here $(f_\hbar)_r^{r+1} = f_\hbar(t_{r+1}) - f_\hbar(t_r)$, $(g_1)_r^{r+1} = g_1(t_{r+1}) - g_1(t_r)$, and $(g_0)_r^{r+1} = g_0(t_{r+1}) - g_0(t_r)$. The wavelet coefficients C_r at each time step can be attained by solving the following equation:

$$\begin{aligned}\boldsymbol{C}_r\left(\boldsymbol{I}^3\boldsymbol{\Psi}(X) - X^2 \otimes \boldsymbol{I}^3\boldsymbol{\Psi}(1)\right) &= -X\frac{(f_\hbar)_r^{r+1}}{\Delta t} - X^2\left[\frac{(g_1)_r^{r+1} - (g_0)_r^{r+1} - (f_\hbar)_r^{r+1}}{\Delta t}\right] \\ &+ \frac{(g_0)_r^t}{\Delta t} - \frac{\alpha}{\hbar}W(X,t_r)^\delta \frac{\partial W}{\partial X}(X,t_r) \\ &+ \frac{\beta}{\hbar^2}\frac{\partial^2 W}{\partial X^2}(X,t_r) - \frac{\gamma}{\hbar^3}\frac{\partial^3 W}{\partial X^3}(X,t_r),\end{aligned} \tag{23}$$

where $\otimes$ stands for the Kronocker product. After substituting the collocation points X_j, $j = 1, 2, \ldots, 2^{k-1}M$, Eq. (23) returns to an algebraic equation which will be solved successively. However, due to the singularity of the obtained matrix on the left-side matrix, an augmented matrix has been solved by elimination to perform the solutions. The numerical solutions are given in Eqs. (13)–(16) are renewed by taking t_{r+1} instead of t.

3 Convergence Analysis

This section is devoted to showing the validation of the proposed method, theoretically. To do this, the convergence issue of the proposed method has been discussed. By taking into account equivalency of the norms in finite spaces, see (Kreyszig 1989 [Theorem 2.4-5]), all theoretical results are presented in L_2-norm. However, before giving the convergence results of the proposed method we first state an important auxiliary lemma such that:

Lemma 1 (*Vichitkunakorn et al. 2020 [Theorem 1]*) *Let $w(X) \in \mathcal{L}^2[0,1]$ such that w is M times differentiable. Let $\boldsymbol{C_r\Psi}(\boldsymbol{x})$ be the best approximation of w in $\Theta = \{\psi_{nm} : 1 \le n \le 2^{k-1},\ 0 \le m \le M-1\}$. Then,*

$$\|w(X,t_r) - \boldsymbol{C_r\Psi}(\boldsymbol{X})\|_2 \le \frac{2^k \max_{\zeta\in[0,1]} w^M(\zeta)}{M!2^{M(k+1)}}. \tag{24}$$

Additionally, due to (Vichitkunakorn et al. 2020 [Theorem 2])

$$\|I^p w(X,t_r) - \boldsymbol{C_r} I^p \boldsymbol{\Psi}(\boldsymbol{x})\|_2 \le \frac{2^k \max_{\zeta\in[0,1]} w^M(\zeta)}{(p-1)!\sqrt{2p(2p-1)}M!2^{M(k+1)}}. \tag{25}$$

Proof The proofs follow the lines of the proofs in Vichitkunakorn et al. (2020) in the case of $h = 1$.

One can be concluded from Lemma 1 that in both cases the right-hand side converges to 0 as k and M increases. Under the lights of Lemma 1, Theorem 1 states the convergence result of the proposed method.

Theorem 1 *Suppose that $w(X,t) : [0,1] \times [0, t_{\text{final}}] \to \mathcal{L}^2[0,1] \cap \mathcal{C}^1[0, t_{\text{final}}]$ is the exact solution and $W(X, t)$ denotes the approximate solution of the transformed equation, Eq. (10). The proposed method described in Sect. 2.1 is convergent in the sense that*

$$\|w(X,t_r) - W(X,t_r)\|_2 \le \|w(X,0) - W(X,0)\|$$

as k, M, and N increase. Here k denotes the division of the spatial domain, M denotes the degree of Taylor wavelet polynomial, and N denotes the number of divisions of the time interval.

Proof The convergence result of the proposed method follows employing the standard technique. To do so, we first, recall the numerical solution and the exact solution as follows:

$$\begin{aligned}W(X,t_{r+1}) &= \Delta t \sum_{n=1}^{2^{k-1}}\sum_{m=0}^{M-1} C_r I^3 \Psi(X) \\ &+ W(X,t_r) + (g_0)_r^{r+1} + X((f_c)_r^{r+1}) \\ &+ X^2\left((g_1)_r^{r+1} - (g_0)_r^{r+1} - (f_c)_r^{r+1} - \Delta t \sum_{n=1}^{2^{k-1}}\sum_{m=0}^{M-1} C_r I^3 \Psi(1)\right)\end{aligned} \tag{26}$$

and

$$w(X,t_{r+1}) = \Delta t \sum_{n=1}^{\infty}\sum_{m=0}^{\infty} C_r I^3 \Psi(X) + w(X,t_r) + (g_0)_r^{r+1} + X((f_c)_r^{r+1}) + X^2\left((g_1)_r^{r+1} - (g_0)_r^{r+1} - (f_c)_r^{r+1} - \Delta t \sum_{n=1}^{\infty}\sum_{m=0}^{\infty} C_r I^3 \Psi(1)\right), \tag{27}$$

where $\Delta t = t_{r+1} - t_r$. Suppose that e_{r+1} denote the error bound at $t = t_{r+1}$, that is $\|e_{r+1}\|_2 = \|w(X,t_{r+1}) - W(X,t_{r+1})\|_2$. By subtracting Eq. (26) from Eq. (27), taking norm of both sides and applying the triangle inequality we have

$$\begin{aligned}\|e_{r+1}\|_2 \le \Delta t \Bigg\| &\sum_{n=1}^{\infty}\sum_{m=0}^{\infty} \boldsymbol{C_r I^3 \Psi}(X) - \sum_{n=1}^{2^{k-1}}\sum_{m=0}^{M-1} \boldsymbol{C_r I^3 \Psi}(X)\Bigg\|_2 \\ &+ \|w(X,t_r) - W(X,t_r)\|_2 \\ &+ X^2 \Delta t \Bigg\| \sum_{n=1}^{\infty}\sum_{m=0}^{\infty} \mathbf{C}_r\left[I^3\Psi(1)\right] - \sum_{n=1}^{2^{k-1}}\sum_{m=0}^{M-1} \mathbf{C}_r\left[I^3\Psi(1)\right]\Bigg\|_2 .\end{aligned} \tag{28}$$

Notice that the boundary conditions are extracted from the exact solution at each time step; thus, the error given in Eq. (28) does not contain any extra terms. With the help of the results of Lemma 1, one can write that

$$\begin{aligned}\|e_{r+1}\|_2 &\le \Delta t \frac{2^k \max_{\zeta\in[0,1]} w^M(\zeta)}{2\sqrt{30}M!2^{M(k+1)}} \\ &\quad + \|e_r\|_2 + X^2 \Delta t \frac{2^k w^M(1)}{2\sqrt{30}M!2^{M(k+1)}}.\end{aligned} \tag{29}$$

More precisely,

$$\|e_{r+1}\|_2 \le \|e_r\|_2 + \Delta t \underbrace{\left(\frac{2^k \max_{\zeta\in[0,1]} w^M(\zeta)}{2\sqrt{30}M!2^{M(k+1)}} + X^2 \frac{2^k w^M(1)}{2\sqrt{30}M!2^{M(k+1)}}\right)}_{\lambda}. \tag{30}$$

Using the relation in Eq. (30) inductively we obtain

$$\begin{aligned}&\|e_1\|_2 \le \|e_0\|_2 + \Delta t\lambda, \\ &\|e_2\|_2 \le \|e_1\|_2 + \Delta t\lambda \le \|e_0\|_2 + 2\Delta t\lambda, \\ &\quad\vdots \\ &\|e_N\|_2 \le \|e_0\|_2 + N\Delta t\lambda,\end{aligned} \tag{31}$$

Notice that as N increases $\Delta t \to 0$. Moreover, as k and M increase $\lambda \to 0$. Thus, one can conclude that

$$\|e_N\|_2 \le \|e_0\|_2 = \|w(X,0) - W(X,0)\|_2. \tag{32}$$

It is crucial to remind that $w(X, t)$ is the exact solution of the transformed equation in Eq. (10), whereas $u(x,t) : [a,b] \times [0, t_{\text{final}}] \to \mathcal{L}^2[a,b] \cap \mathcal{C}^1[0, t_{\text{final}}]$ stands for the exact solution of the main equation in Eqs. (1), (2). Using the fact that $w(X,t) = u(x,t)$ one can be said $W(X,t) = U(x,t)$ where $W(X, t)$ and $U(x, t)$ denotes the approximate solutions of the transformed equation and the main equation, respectively. Thus, one can be concluded by the result in Eq. (31) the proposed method tends to converge to the exact solution, that is $U(x,t) \to u(x,t)$ when k, M, and N increases.

4 Numerical Examples and Simulations

In numerical analysis, even though the theoretical analysis has shown that the proposed method converges to the exact solution, there can occur some problems in computation due to the compelling structures. Therefore, the theoretical results are required to confirm computationally. The objective of this section is to check the validity and efficiency of the proposed method for the KdV–Burgers equation and modified KdV equation.

All numerical results have been recorded by applying the proposed method to the transformed equation with appropriate choices of parameters. Moreover, the results have been produced by collocating a suitable number of Newton–Cotes nodes

$$X_j = \frac{2j-1}{2^k M}, \quad j = 1, 2, \ldots, 2^{k-1}M. \tag{33}$$

Additionally, the accuracy of the method is tested at the final time, t_{final}, with the L_∞ and L_2 norms:

$$\|u - U\|_{L_\infty} = \max_i |u(x_i, t_{\text{final}}) - U(x_i, t_{\text{final}})|,$$

$$\|u - U\|_{L_2} = (\Delta x \sum_{i=0}^{N} (u(x_i, t_{\text{final}}) - U(x_i, t_{\text{final}}))^2)^{1/2},$$

where $u(x, t)$ and $U(x, t)$ represent the exact solution and numerical solution, respectively. Furthermore, all computations have been executed on Intel Core, i7-6700HQ 2.60Ghz and 16GB of RAM and implemented via the MATLAB-2018b programming language.

Example 1 As a first example, Eq. (1) is considered over the domain $x \in \Omega = [-20, 20]$ and $t \in [0, t_{\text{final}}]$. The exact solution of the equation is

$$u(x,t) = \frac{-6\beta^2}{25\gamma\alpha}\left[1 + \tanh\left(\frac{\beta}{10\gamma}\left(x + \frac{6\beta^2}{25\gamma}t\right)\right) - \frac{1}{2}\operatorname{sech}^2\left(\frac{\beta}{10\gamma}\left(x + \frac{6\beta^2}{25\gamma}t\right)\right)\right].$$

Table 1 Comparison of errors of Example 1 in L_∞ norm

t_{final}	Proposed method	EXP-MQ (Koçak 2021)	B-spline (Hepson et al. 2019)	MQ (Haq et al. 2009)
1	9.690e−19	4.404e−11	7.271e−11	6.822e−09
10	1.011e−17	1.995e−08	9.509e−11	2.479e−08

The recorded results are computed by taking $\alpha = 1,\ \delta = 1,\ \beta = 0.004$ and $\gamma = 0.1$ for different choices of t_{final} values. The domain $x \in [-20, 20]$ is collocated by 16 number of points by taking $k = 3,\ M = 4$

Table 2 Comparison of errors of Example 1 in L_∞ and L_2 norms where $k = 3$ and $M = 4$

β	t_{final}	Proposed method		EXP-MQ (Koçak 2021)		MQ (Haq et al. 2009)	
		L_∞	L_2	L_∞	L_2	L_∞	L_2
$\beta = 0.04$	1	7.912e−14	2.685e−13	2.234e−07	2.781e−07	2.936e−06	3.727e−07
	10	2.829e−11	5.321e−11	2.950e−06	5.833e−06	5.800e−06	1.297e−05
$\beta = 0.1$	1	8.444e−09	2.302e−08	6.605e−06	6.269e−06	1.540e−05	1.004e−05
	10	2.906e−06	5.402e−06	2.955e−05	3.762e−05	1.498e−04	1.342e−04

The recorded results are computed by taking $\alpha = 1,\ \delta = 1$, and $\gamma = 0.1$ for different choices of β and t_{final} values where $x \in [-20, 20]$ and $\Delta t = 0.001$.

The initial and boundary conditions are taken from the exact solution.

The proposed method has been tested on the specified equation. The results of Table 1 have been computed by taking the parameters $\alpha = 1,\ \delta = 1,\ \beta = 0.004$, and $\gamma = 0.1$ over different final times where $\Delta t = 0.001$. The recorded results are compared to exponential Rosenbrock integrator combined with meshfree method (EXP-MQ) in Koçak (2021), extended B-spline collocation method (B-spline) in Hepson et al. (2019), and a mesh-free method combined by the Crank-Nicolson method (MQ) in Haq et al. (2009). For a reliable comparison, the accuracy of the proposed method in $L_\infty-$ norm is listed in Table 1.

The elapsed time of obtaining the numerical solution by the proposed method is 2.03 s for $t_{\text{final}} = 1$ and 20.68 s for $t_{\text{final}} = 10$. Besides Table 1, Table 2 also promotes how well the proposed method fit the exact solution in both L_∞ and L_2 errors. The listed errors of Table 2 are obtained by considering $\alpha = 1,\ \delta = 1$, and $\gamma = 0.1$ for different values of β.

The maximum elapsed time for performing the data in Table 1 has been recorded for almost 23 s for $\beta = 0.1$ and $t_{\text{final}} = 10$.

Tables 1 and 2 guarantee that the proposed method has achieved better results than the existing literature. The compared studies have used the 4th-order Runge–Kutta which is a higher-order method, the Crank–Nicolson method which is a semi-implicit solver, and the exponential Rosenbrock method which is a kind of stiff solver on their temporal domain. It is crucial to highlight that even though the proposed method has used a fewer rate of convergence without possessing any property, by virtue of the success of the Taylor wavelet method, the proposed method has recorded better results than those in the literature.

Table 3 Errors of conserved quantities of Example 1 in L_∞ norm where $k = 3$ and $M = 4$

β	t_{final}	$\|C_1 - \tilde{C_1}\|$	$\|C_2 - \tilde{C_2}\|$	$\|C_3 - \tilde{C_3}\|$
0.004	1	6.346e−09	7.326e−13	4.517e−10
	3	6.346e−09	7.326e−13	4.517e−10
	10	6.346e−09	7.326e−13	4.517e−10
0.04	1	2.971e−05	3.927e−07	3.614e−04
	3	2.969e−05	3.927e−07	3.615e−04
	10	2.963e−05	3.925e−07	3.617e−04
0.1	1	8.422e−05	7.948e−06	4.408e−02
	3	8.310e−05	7.854e−06	4.408e−02
	10	7.161e−05	6.893e−06	4.409e−02

The recorded results are computed by taking $\alpha = 1,\ \delta = 1$, and $\gamma = 0.1$ for different choices of β and t_{final} values where $x \in [-20, 20]$ and $\Delta t = 0.001$

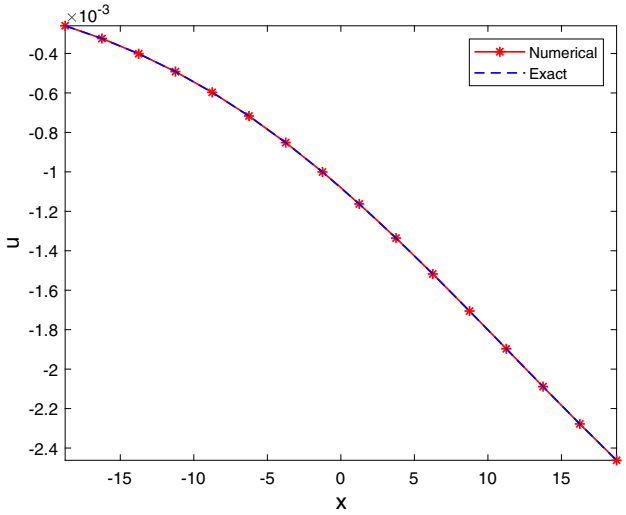

(a) $\alpha = 1,\ \delta = 1,\ \gamma = 0.1$ and $\beta = 0.03$.

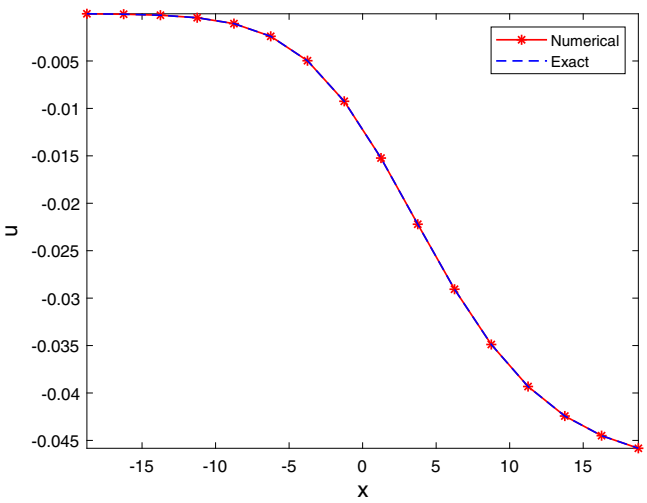

(b) $\alpha = 1,\ \delta = 1,\ \gamma = 0.1$ and $\beta = 0.1$.

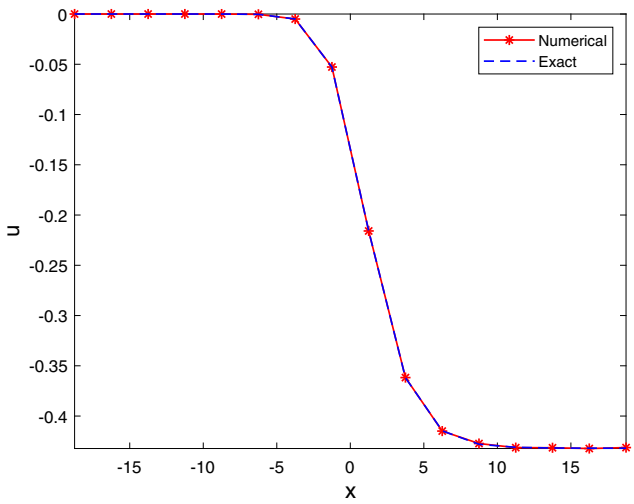

(c) $\alpha = 1,\ \delta = 1,\ \gamma = 0.1$ and $\beta = 0.3$.

Fig. 1 The physical behaviors of the numerical solution and the exact solution of Example 1 at $t_{\text{final}} = 1$ for various choices of β. The results are recorded for $k = 3$ and $M = 4$

Moreover, it is known that the KdV–Burgers equation preserves various dynamical quantities such as mass, momentum, and energy conservations. To examine the validity of the proposed method, the following conservative values have also been confirmed:

$$C_1 = \int_{-20}^{20} u(x, t_{\text{final}})\,\mathrm{d}x, \tag{34}$$

$$C_2 = \int_{-20}^{20} u^2(x, t_{\text{final}})\,\mathrm{d}x, \tag{35}$$

$$C_3 = \int_{-20}^{20} [u^3(x, t_{\text{final}}) - 3\frac{\gamma}{\alpha}(u_x)^2(x, t_{\text{final}})]\mathrm{d}x \tag{36}$$

where C_1 corresponds to mass, C_2 corresponds to momentum and C_3 corresponds to energy. In discrete space, conserved quantities are computed as follows:

$$\tilde{C_1} = \Delta x \sum_{i=1}^{N} U(x_i, t_{\text{final}}), \tag{37}$$

$$\tilde{C_2} = \Delta x \sum_{i=1}^{N} (U(x_i, t_{\text{final}}))^2, \tag{38}$$

$$\tilde{C_3} = \Delta x \sum_{i=1}^{N} (U(x_i, t_{\text{final}}))^3 - 3\frac{\gamma}{\alpha}(U_x(x_i, t_{\text{final}}))^2. \tag{39}$$

Table 3 demonstrates the maximal errors of mass, momentum, and energy of the proposed method. For obtaining errors, the parameters of the specified equation

Table 4 Comparison of errors of Example 2 in L_∞ norm where $k = 3$ and $M = 3$

x	$\gamma = -0.001$		$\gamma = -0.1$	
	Proposed method	HWM (Ray and Gupta 2015)	Proposed method	HWM (Ray and Gupta 2015)
0.03125	1.90656e−13	1.72895e−07	9.74922e−10	1.27575e−05
0.09375	2.21456e−13	1.55692e−06	8.59581e−09	1.16031e−04
0.15625	8.59904e−13	4.33497e−06	2.37119e−08	3.33334e−04
0.21825	3.50268e−12	8.53102e−06	4.59690e−08	6.90107e−04
0.28125	9.79544e−12	1.41814e−05	7.45945e−08	1.22625e−04
0.34375	7.59551e−12	2.13321e−05	9.79432e−08	1.99484e−03
0.40625	2.17469e−12	3.00363e−05	1.17568e−07	3.00363e−03
0.46875	2.83105e−12	4.03506e−05	1.33316e−07	4.49462e−03
0.53125	3.37478e−12	5.23326e−05	1.47358e−07	6.37673e−03
0.59375	3.82871e−12	6.60379e−05	1.49658e−07	8.78725e−03
0.65625	4.67586e−12	8.15183e−05	1.41185e−07	1.18068e−02
0.71875	6.05539e−12	9.88196e−05	1.23554e−07	1.55134e−02
0.78125	8.56088e−12	1.17981e−04	9.92058e−08	1.99805e−02
0.84375	7.96186e−12	1.39034e−04	7.20468e−08	2.52756e−02
0.90625	5.62666e−12	1.62005e−04	4.31693e−08	3.14593e−02
0.96875	1.90895e−12	1.86910e−04	1.44035e−08	3.85831e−02

The recorded results are computed by taking $\alpha = 6$, $\delta = 2$, and $\beta = 0$ for different choices of γ values where $x \in [0, 1]$, $t_{\text{final}} = 1$ and $\Delta t = 0.0001$

are chosen as $\alpha = 1$, $\delta = 1$, and $\gamma = 0.1$ for various values of β. The physical domain is fixed, that is $x \in [-20, 20]$, whereas the time interval has been varied by taking different final time values.

The values in Table 3 are evidence that the proposed method preserves the important dynamical quantities. Furthermore, to check the applicability of the proposed method on the structural behavior Fig. 1 is depicted. For the exhibited figure, Example 1 has been studied in accordance with the previous works in Haq et al. (2009), Hepson et al. (2019), Koçak (2021), that is, the parameters are chosen as $\alpha = 1$ and $\gamma = 0.1$ for different choices of β values.

Figure 1 shows that the proposed method preserves the structural behavior. With the help of Fig. 1 and Table 3, one can conclude that the proposed method has provided

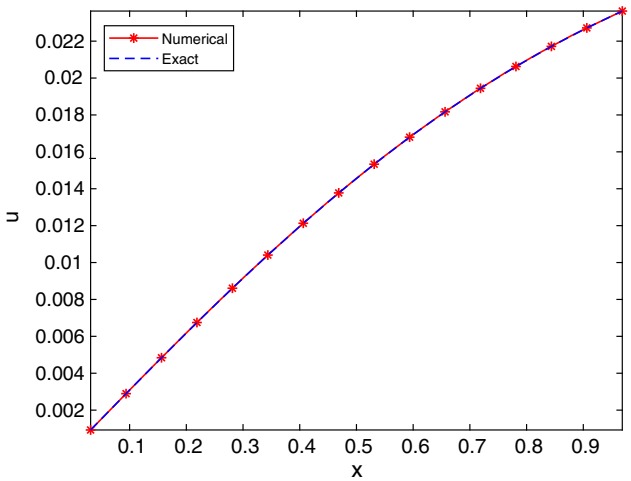

(a) Comparison of numerical solution and exact solution at $t_{final} = 1$ where $\gamma = -0.001$

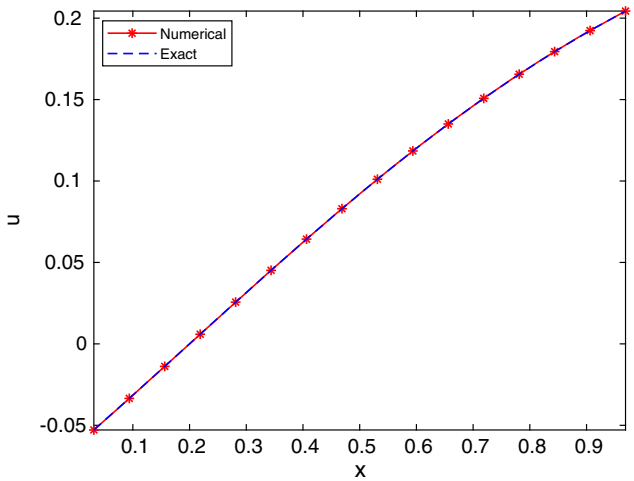

(b) Comparison of numerical solution and exact solution at $t_{final} = 1$ where $\gamma = -0.1$

Fig. 2 The physical behaviors of the numerical solution and the exact solution of Example 2 at $t_{\text{final}} = 1$ for different choices γ where $\alpha = 6$. The results are exhibited for $k = 3$ and $M = 8$

physical compatibility by preserving all nature of Example 1.

Example 2 To compare the proposed method to the existing wavelet literature, the modified-KdV equation is studied as our next problem. This means that Eq. (1) is studied on $x \in \Omega = (0, 1)$ by fixing $\delta = 2$ and $\beta = 0$. The exact solution of the specified equation is defined as follows:

$$u(x,t) = \sqrt{\frac{-6\gamma}{\alpha}}\tanh(x + 2\gamma t).$$

It is noted that all required conditions are chosen from the exact solution.

The main reference to compare the results obtained by the proposed method is Ray and Gupta (2015). Table 4 presents the comparison of the recorded L_∞ errors of the proposed method and the Haar wavelet method in Ray and Gupta (2015).

Table 4 emphasizes that the proposed method has recorded better solution than those in Ray and Gupta (2015). Moreover, the CPU time of the proposed method is discussed. The maximum elapsed times of the proposed method for $t \in [0, 1]$ are 29.67 and 27.55 in s for $\gamma = -0.001$ and $\gamma = -0.1$, respectively. In addition to Table 4, the applicability has been confirmed on the physical behavior which is illustrated in Fig. 2. To do so, Example 2 is solved by taking $\alpha = 6,\ \Delta t = 0.0001$ and collocating 16 points.

Figure 2 guarantees the physical compatibility of the proposed method with the exact solution.

5 Conclusion

The presented study has focused on proposing a reliable, accurate, and efficient numerical solution for both KdV–Burgers' and modified-KdV equations which are kind of challenging problems in applied sciences. The proposed method has essentially based on the combination of the Taylor wavelet collocation method in the spatial domain and the explicit Euler method in the temporal domain. After ensuring the convergence of the proposed method theoretically, the computational work has been efforted. The numerical section of the study has been enriched by testing the proposed method on benchmark problems. The outcomes of the study can be underlined as follows: not only the proposed method has obtained highly accurate results when compared to the exact solution but also the recorded errors have achieved the best records when compared to those reported in the literature. Besides its accuracy, unlike the other studies, the computational cost of the proposed method to return a numerical solution has been performed. Additionally, the exhibited figures are also evident that the proposed method is compatible with the exact solution, physically. Furthermore, the proposed method has also been validated via the qualitative properties of the equations. All presented results have been shown that the proposed method has solved the specified equations by preserving the nature of the problem.

Acknowledgements The authors would like to thank the reviewers and the Editor-in-Chief for their contribution to progress of the study by constructive, valuable, and insightful comments to this study.

Author contributions The whole work has been provided by all authors. That is, SOK and NIK were involved in conceptualization, methodology, analysis, MATLAB codding, writing—original draft, writing-review and editing.

Funding The authors received no specific funding for the current work.

Declarations

Conflict of interest The authors declare that they have no conflict of interest.

References

Ak T, Karakoc SBG, Biswas A (2017) An approach based on a lumped Galerkin method via cubic B-spline interpolation. Iran J Sci Technol Trans Sci Trans A Sci 41:1109–1121. https://doi.org/10.1007/s40995-017-0238-5

Aydin A (2015) An unconventional splitting for Korteweg de Vries-Burgers equation. Eur J Pure Appl Math 8(1):50–63

Darvishi MT, Khani F, Kheybari S (2007) A numerical solution of the KdV–Burgers equation by spectral collocation method and Darvishi's preconditionings. Int J Contemp Math Sci 2(22):1085–1095

Dehestani H, Ordokhani Y, Razzaghi M (2019) On the applicability of Genocchi wavelet method for different kinds of fractional-order differential equations with delay. Numer Linear Algebra Appl 26(5):e2259. https://doi.org/10.1002/nla.2259

Dehestani H, Ordokhani Y, Razzaghi M (2021) Combination of Lucas wavelets with Legendre–Gauss quadrature for fractional Fredholm–Volterra integro-differential equations. J Comput Appl Math. https://doi.org/10.1016/j.cam.2020.113070

Dehestani H, Ordokhani Y, Razzaghi M (2021) Modified wavelet method for solving multitype variable-order fractional partial differential equations generated from the modeling of phenomena. Math Sci. https://doi.org/10.1007/s40096-021-00425-1

Dehestani H, Ordokhani Y, Razzaghi M (2021) A novel direct method based on the Lucas multiwavelet functions for variable-order fractional reaction-diffusion and subdiffusion equations. Numer Linear Algebra Appl 28(2):e2346. https://doi.org/10.1002/nla.2346

Haq S, Islam S, Uddin M (2009) A mesh-free method for the numerical solution of the KdV-Burgers equation. Appl Math Model 33(8):3442–3449. https://doi.org/10.1016/j.apm.2008.11.020

Hepson OE, Korkmaz A, Dağ I (2019) Extended B-spline collocation method for KdV–Burgers equation. TWMS J Appl Eng Math 9(2):267–278

Irk D (2017) Quinctic B-spline Galerkin method for the KdV equation. Anadolu Univ J Sci Technol B Theor Sci 5(2):111–119. https://doi.org/10.20290/aubtdb.289203

Kaya D (2009) Semi-analytical methods for solving the Korteweg–de Vries equation (KdV) and modified Korteweg–de Vries equations (mKdV). In: Meyers R (ed) Encyclopedia of complexity and systems science. Springer, New York, NY, pp 5144–5160. https://doi.org/10.1007/978-0-387-30440-3_305

Keshavarz E, Ordokhani Y, Razzaghi M (2018) The Taylor wavelets method for solving the initial and boundary value problems of Bratu-type equations. Appl Numer Math 128:205–216. https://doi.org/10.1016/j.apnum.2018.02.001

Keshavarz E, Ordokhani Y (2019) A fast numerical algorithm based on the Taylor wavelets for solving the fractional integro-differential equations with weakly singular kernels. Math Methods Appl Sci 42(13):4427–4443. https://doi.org/10.1002/mma.5663

Koçak H (2021) A combined meshfree exponential Rosenbrock integrator for the third-order dispersive partial differential equations. Numer Methods Partial Differ Equ 37:2458–2468. https://doi.org/10.1002/num.22726

Kreyszig E (1989) Introductory functional analysis with applications. Wiley, New York

Kumar B, Priyadarshi G (2018) Wavelet Galerkin method for fourth-order multi-dimensional elliptic partial differential equations. Int J Wavelets Multiresolut Inf Process 16:1850045:1-1850045:25. https://doi.org/10.1002/num.22726

Motsa SS, Magagula VM, Sibanda P (2014) A bivariate chebyshev spectral collocation quasi linearization method for nonlinear evolution parabolic equations. Sci World J 2014, Article ID 581987. https://doi.org/10.1155/2014/581987

Priyadarshi G, Kumar BVR (2020) Reconstruction of the parameter in parabolic partial differential equations using Haar wavelet method. Eng Comput 38(5):2415–2433. https://doi.org/10.1108/EC-03-2020-0163

Ratas M, Salupere A (2020) Application of higher order Haar wavelet method for solving nonlinear evolution equations. Math Model Anal 25(2):271–288. https://doi.org/10.3846/mma.2020.11112

Ray SS, Gupta AK (2015) An approach with Haar Wavelet collocation method for numerical simulations of modified KdV and modified Burgers equations. Comput Model Eng Sci 103(5):315–341

Saleem S, Hussain MZ, Aziz I (2021) A reliable algorithm to compute the approximate solution of KdV-type partial differential equations of order seven. PLoS ONE 16(1):Article Id:e0244027. https://doi.org/10.1371/journal.pone.0244027

Shi Y, Xu B, Guo Y (2015) Numerical solution of Korteweg-de Vries–Burgers equation by the compact-type CIP method. Adv Differ Equ 2015:Article ID 353. https://doi.org/10.1186/s13662-015-0682-5

Vichitkunakorn P, Vo TN, Razzaghi M (2020) A numerical method for fractional pantograph differential equations based on Taylor wavelets. Trans Inst Meas Control 42(7):1334–1344. https://doi.org/10.1177/0142331219890171